[CANCER RESEARCH 63, 4705–4712, August 1, 2003]

Effect of Longitudinal Oxygen Gradients on Effectiveness of Manipulation of Tumor Oxygenation[1,2]

Kristian Erickson, Rod D. Braun, Daohai Yu, Jennifer Lanzen, David Wilson, David M. Brizel, Timothy W. Secomb, John E. Biaglow, and Mark W. Dewhirst[3]

Departments of Radiation Oncology [K. E., R. D. B., J. L., D. M. B., M. W. D.] and Biostatistics and Bioinformatics [D. Y.] Duke University Medical Center. Durham, North Carolina 27710; Departments of Biochemistry and Biophysics [D. W.] and Radiation Oncology [J. E. B.], University of Pennsylvania Philadelphia, Pennsylvania; and Department of Physiology University of Arizona, Tucson, Arizona [T. W. S.]

ABSTRACT

The purpose of this study was to test the hypothesis that longitudinal O_2 gradients in tumor affect response to manipulation of oxygenation. Previously we showed that pO_2 is higher on the fascial than the tumor surface of the R3230Ac rat mammary carcinoma when growing in a dorsal skin-fold window chamber, reflecting a longitudinal oxygen gradient. Magnetic resonance angiography verified prior results: the fascial surface has arterioles and higher vascular density than tumor; and the tumor surface has no arterioles. Phosphorescence lifetime imaging was used to measure each surface hypoxic percentage (HP; percentage of pixels < 10 mm Hg) before and after administration of mannitol or glucose (1 g/kg, i.v.) followed by O_2 breathing. The fascial surface had a smaller HP (median = 2.72%) than tumor (median = 27.94%; $P = 0.0002$) at baseline. HP on the fascial surface was positively correlated with HP on the tumor surface ($P = 0.0067$). HP decreased on the fascial surface after either sugar + O_2 (mannitol $P = 0.03$; glucose $P = 0.06$; combined $P = 0.002$), but HP did not change on the tumor surface. Therefore, the tumor surface is refractory to improvement in pO_2 with this method. Additional refinements may be needed to improve pO_2 of analogous regions in larger tumors; mechanism-driven suggestions are provided.

INTRODUCTION

Chronic tumor hypoxia, a significant mechanism for tumor radioresistance, has traditionally been thought to result from limitations of oxygen gradients in the radial direction from blood vessels (1–3). In recent studies using skin-fold window chamber tissues, we have demonstrated a decline in pO_2 with distance from the fascial plane beneath the growing tumor, *i.e.*, in the longitudinal direction with respect to the arterioles that supply the tumor (4). Over a distance of 200 μm from the fascial surface to the tumor surface, the HP[4] increases 5-fold. There is also a 20 mm Hg difference in vascular pO_2 between the two surfaces (as measured with oxygen microelectrodes), along with measurable gradients in glucose and lactate concentrations that reflect a transition from aerobic to anaerobic metabolism (5, 6). Separate studies measuring the effects of glucose and oxygen breathing on tumor oxygenation in the same tumor growing in the flank show that regions with low initial pO_2 levels exhibit smaller increases in pO_2 after treatment than regions with higher baseline pO_2 levels (7). We therefore hypothesized that the tumor surface of the chamber preparation might represent those regions that are refractory to oxygenation because blood reaching such regions must first pass through moderately hypoxic tissue where most of the oxygen in the blood may be extracted.

The logic for combining hyperglycemia with hyperoxia comes from the observation that moderate levels of hyperglycemia are capable of inducing a relative shift from respiration to glycolysis in tumor cells via the Crabtree effect, thus decreasing tumor oxygen consumption (7–9). Theoretical models suggest that reduction of oxygen consumption combined with increased oxygen delivery should be very effective in improving oxygen delivery to tumors (10, 11), and we have recently verified this prediction in the tumor model that was evaluated for this study (7). Recent human clinical studies examining the combination of glucose and oxygen breathing on tumor pO_2 have also been impressive (D. Brizel, unpublished data).

We hypothesized that improvements in tumor pO_2 would differ markedly when comparing the tumor to the fascial surface and that use of glucose with oxygen breathing would be better than mannitol (a nonmetabolizable sugar) with oxygen breathing. PLI was used to measure oxygenation of the fascial and tumor surfaces of these windows at baseline and after manipulation of oxygen transport with sugar followed by oxygen breathing.

MATERIALS AND METHODS

Animal Model. R3230Ac mammary adenocarcinomas were grown in the dorsal skin flap window chamber of Fisher 344 rats (100–150 g). The rats were surgically implanted with anodized aluminum window chambers as described previously (12). A small piece of tumor from a donor animal (0.1 mm^3) was transplanted onto the fascia at the time of surgery. Glass windows were placed on both sides of the chamber to provide visual access and to protect the tissue. Before and after implantation, the animals were kept in an environmental chamber at DUMC maintained at 34°C and 50% humidity. Lighting procedures were standard, and food and water were provided *ad libitum*. After sufficient tumor growth (9–11 days after transplantation), the animals were shipped from DUMC to the University of Pennsylvania, where PLI imaging was carried out within 4 days of animal arrival. All protocols were approved by the DUMC and University of Pennsylvania Institutional Animal Care and Use Committees.

Anesthesia. Animals were anesthetized with i.p. sodium pentobarbital (50 mg/kg) for all surgical and experimental procedures. For the experimental measurements of tissue oxygenation, blood pressure was monitored using a digital manometer (Digi-Med Blood Pressure Analyzer Model 190; Micro-Med, Louisville, KY), and body temperature was maintained with either heated paraffin pads or temperature-controlled water blankets (T/Pump; Gaymar Industries, Inc., Orchard Park, NY).

PLI. After infusion with 60 mg/ml Pd-mesotetra-(4-carboxyphenyl)-porphyrin (Oxyphore), a gated, intensified CCD camera was used to image phosphorescence from the upper and lower window surfaces. Blue light (419 nm) excitation flashes were made at both surfaces, and the camera was turned on at various times after the excitation flash. The porphyrin compound has an absorption peak at this wavelength, and the blue light penetrates to ~50 μm in the tissue. Details of these methods have been published previously (13–15).

Experimental Protocol. At the beginning of each experiment, animals were anesthetized, and a femoral artery and vein were cannulated for respective measurements of arterial blood pressure and i.v. infusion of drugs/glucose. Animals were then placed on a heated paraffin pad and positioned under an operating microscope equipped with a 419-nm light source and a CCD camera.

Received 1/23/03; accepted 5/21/03.

The costs of publication of this article were defrayed in part by the payment of page charges. This article must therefore be hereby marked *advertisement* in accordance with 18 U.S.C. Section 1734 solely to indicate this fact.

[1] This work was supported by NIH/National Cancer Institute Grants CA40355 (to M. W. D.) and NS-31465 (to D. W.) and a Howard Hughes Foundation Fellowship (to K. E.).

[2] Supplementary data for this article is available at *Cancer Research Online* (http://cancerres.aacrjournals.org).

[3] To whom requests for reprints should be addressed, at Box 3455, Duke University Medical Center, Durham, NC 27710. Phone: (919) 684-4180; Fax: (919) 684-8718; E-mail: dewhirst@radonc.duke.edu.

[4] The abbreviations used are: HP, hypoxic percentage; PLI, phosphorescence lifetime imaging; CCD, charged coupled device; DUMC, Duke University Medical Center.

The oxyphore solution (0.2 ml) was administered i.v., which typically resulted in a transient increase in blood pressure for a few minutes (average maximum increase of 16% within 1 min from an average baseline of 108 mm Hg). Once blood pressure returned to baseline (mean, 5.5 min), the tumor was imaged on both sides of the window chamber. The initial side imaged was determined by randomization. After the initial imaging was completed (10–20 min after the Oxyphore infusion), the venous catheter was attached to an infusion pump, and 1 g/kg of either glucose or mannitol was infused over 7–8 min (200 mg/ml at a rate of 0.1 ml/min). Halfway through this infusion, the skin window was imaged on the tumor surface side. At the end of the glucose or mannitol infusion, the venous line was removed from the pump and was flushed with heparinized saline. Nine min after completing the glucose or mannitol infusion, a facemask was placed over the snout of the animal, and either air or 100% oxygen was delivered. Beginning 1 min later, the chamber was imaged again on both sides.

Image Analysis for PLI. The phosphorescence lifetime images yielded a map of vascular oxygenation at the defined points during the experiment, and the phosphorescence signal intensity exhibited little decay for at least 1 h after injection. Each PLI image was converted into a histogram, from which oxygen distribution data were extracted. The PLI technique is most accurate for measurement of oxygen levels < 40 mm Hg. Oxygen levels of at least some portion of each of the fascial surfaces were frequently >40 mm Hg after treatment. Therefore, we used HP (percentage of pixels in the imaged surface with $pO_2 < 10$ mm Hg) as a measure of tissue hypoxia.

Magnetic Resonance Microscopy. In a separate group of animals, three-dimensional visualization of tumor vascular geometry was performed using magnetic resonance microscopy. GdAlbumin was administered as a contrast agent in a manner similar to that reported previously (4). Briefly, rats were anesthetized with sodium pentobarbital (50 mg/kg), the upper glass was removed from the window chamber and was suffused with PBS. BSA diethylenetriaminepentaacetic anhydride-gadolinium was injected i.v. in a volume of 1.0 ml (containing 1 mM Gd). Fifteen s after injection, the skin flap was immersed in 10% buffered formalin and was then removed from the animal. After embedding in agarose (3%), the tissue was imaged in a 1-cm solenoid imaging coil. Imaging was performed on a 9.4T Oxford Instruments magnet. Data were acquired using three-dimensional spin warp encoding. The pixel array was 256 (3), with pixels of 40 μm on a side. The repetition time was 200 ms, and the echo time was 6 ms. Four excitations were taken for each encoding step.

Statistical Analysis. Data on a total of 17 animals in three treatment groups were collected and available for the data analysis. Measurements were made at two locations in the tumor model: the fascial and tumor surfaces. The two treatment groups were mannitol + oxygen ($n = 7$) and glucose + oxygen ($n = 6$). An additional 4 animals were imaged on the tumor and fascial surfaces but were not analyzed for response to manipulation. There were two experiments where measurements were not taken of the tumor surface after the end of the sugar infusion because of technical constraints. However, there were data obtained after the onset of oxygen breathing in both of these experiments. These experiments were included in the analyses involving evaluation of baseline HP and after initiation of oxygen breathing. Comparisons between values obtained from the two surfaces at baseline and changes in a given surface HP in response to manipulation were made using the signed rank test. Comparisons between some parameters were made using simple linear regression.

RESULTS

Images obtained from magnetic resonance angiograms of window chamber tumors are shown in Fig. 1. The fascial and tumor surfaces are shown from one tumor (Fig. 1, *A* and *B*). The tumor margin is indicated by a mound of microvessels emerging from the underlying fascial layer. The caliber of vessels is much higher on the fascial surface. The fact that they are so readily visible means that they are >40 μm in diameter, which is the pixel dimension for this image. Images are shown *en face* at three different depths in another tumor (Fig. 1*C*). The vasculature of the tumor surface and the deep tumor margin (adjacent to the fascia) are more visible than that seen in the

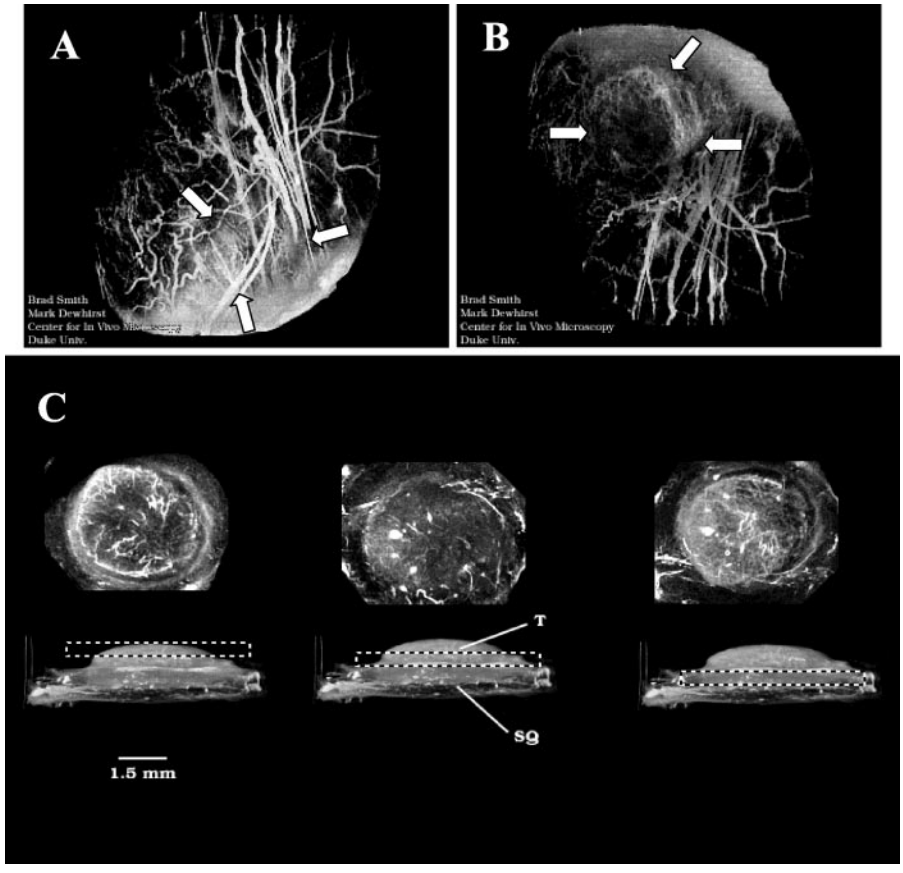

Fig. 1. High-resolution magnetic resonance GdAlbumin angiography of window chamber tumors. *A*, full thickness image of window, as viewed from the fascial surface. Many high caliber vessels are seen on the fascial surface. From intravital microscopy studies, it is known that some of these vessels are arterioles that supply blood to the tumor (21). Location of underlying tumor is indicated by *arrows*. *B*, same tumor as in *A*, viewed from the tumor surface. The tumor grows as a mound from the underlying fascia. Margins are indicated by the *arrows*. *C*, planar images at different depths in another tumor. The location of each plane is indicated in cross section. The vascular density of the tumor, adjacent to the fascial surface and the tumor surface itself, is higher than in the interior of the tumor. T = tumor, SQ = s.c. (fascial) surface. Note that the thickness of the tumor is >250 μm in this image. This occurs because the tumor tissue typically swells when a coverglass is removed and replaced with a suffusion medium. The fascia also appears thicker than it is in the intact chamber as well. In histological sections, this layer is typically no more than 10–20-μm thick (data not shown).

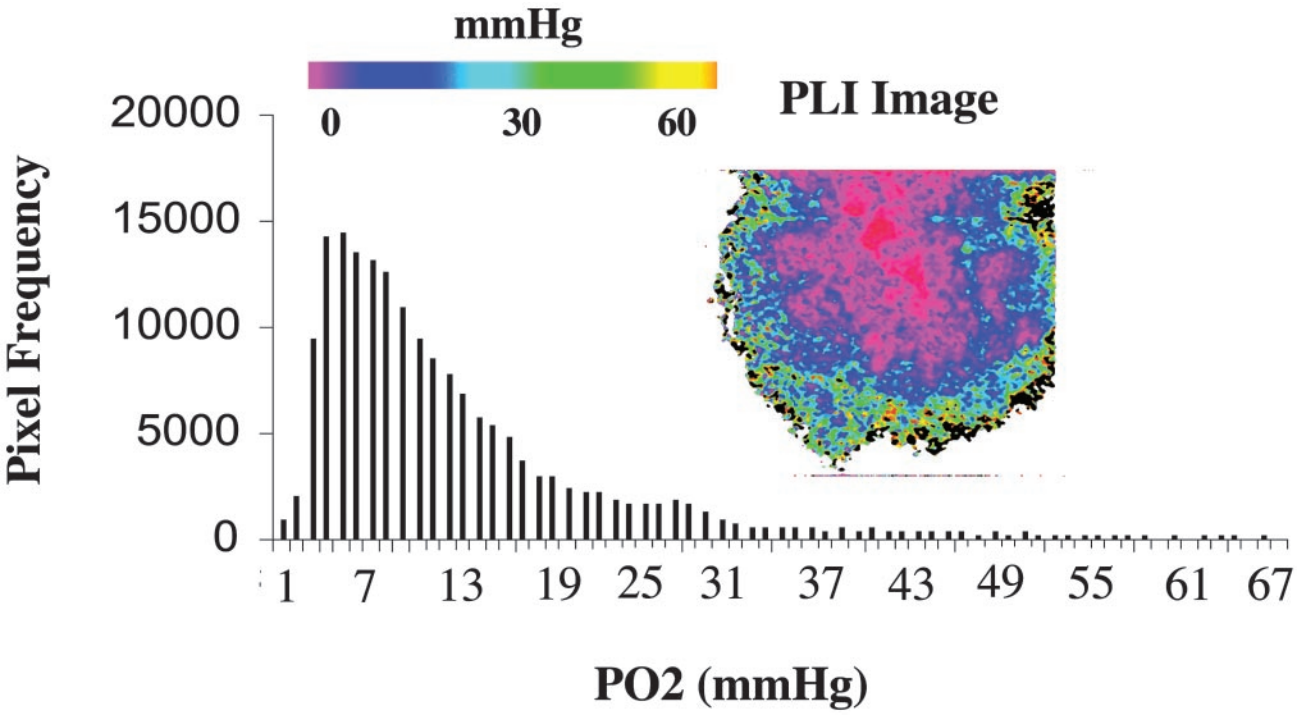

Fig. 2. Samples of a phosphorescence lifetime image and pixel-pO_2 histogram. These data were acquired from the tumor surface of a window chamber preparation under air breathing conditions. The *color bar* indicates color range *versus* pO_2.

interior of the tumor. Vessels of the fascial layer are not as clear *en face* in this example. This is probably because many vessels in the fascia are <40 μm, which is the pixel dimension of the images. Because these tumors are devoid of fascia on one side, they have arteriolar input from one side only, as we have documented previously using intravital microscopy (5, 16). It is important to note that the term fascial surface in this model does not imply that there is a thick layer of normal tissue on this surface. Prior histological studies have shown that this surface is composed primarily of a thin layer of collagen (sometimes admixed with tumor cells) that contains tumor feeding vasculature and other microvessels (6). The PLI method measures signal up to 50 μm in depth; thus, the signal is dominated by the tumor cells that are deep to the fascial layer (4).

A phosphorescence lifetime image, taken at baseline, is shown in Fig. 2, along with a representative pO_2 histogram. The histogram data were used to establish the percentage of hypoxic pixels for each surface imaged. Fig. 3 shows an example of results for an animal treated with mannitol and oxygen breathing. Baseline images are shown as well as images taken 10 min after the start of oxygen breathing, following the protocol outlined in "Materials and Methods." The tumor surface is more hypoxic than the fascial surface. Upon oxygen breathing, HP is clearly decreased on the fascial surface, whereas the HP of the tumor surface appears to actually increase.

Comparison of HP between Fascial and Tumor Surfaces at Baseline. The median baseline HP was 28% on tumor surfaces compared with 2.7% on fascial surfaces (Table 1). In all experiments, the HP on the tumor surface was greater than or equal to the percentage on the fascial surface; the median of the differences was 25%, which was significant ($P = 0.0002$). There was no significant difference in baseline HP between the mannitol- and glucose-treated groups on the fasical surfaces. On the tumor surfaces, the glucose group tended to have a higher median HP (median = 55.6% with a range from 8.5 to 43.8%), compared with the mannitol group (median = 14.6% with range from 7.0 to 82.3%). This difference was not significant. There was a positive relationship between baseline HPs on the tumor *versus* fascial surfaces (linear regression; $r = 0.63$, $F = 9.86$, $P = 0.0067$; Fig. 4). This observation can be interpreted to mean that there was variation in the overall oxygenation state between individual tumors. For example, when the tumor surface was relatively hypoxic compared with other experiments, the fascial side tended to be relatively hypoxic also.

Change in HP of the Tumor Surface after Administration of Sugar. The HP remained virtually unchanged on the tumor surface from baseline *versus* after sugar administration (Tables 2 and 3). For mannitol, the HP rose slightly by 2.3%, but this difference was not significant ($P = 0.56$). For glucose, the HP dropped slightly by 6.3%, but again, the difference was not significant ($P = 0.44$).

Change in HP of Each Surface after Sugar and during O_2 Breathing. Treatment with sugar followed by oxygen breathing led to significant declines in HP on the fascial surface. For mannitol, the HP dropped from a median of 6.0 to 0.4% (Tables 2 and 3), a difference which was significant ($P = 0.03$). A trend toward significance was seen for glucose, with the median dropping by 12.6% ($P = 0.06$). The data for mannitol and glucose did not differ significantly ($P = 0.95$) and were therefore combined for additional evaluation. In the combined data, the average HP on the fascial surface declined significantly from a median value of 6.1 to 0.5% ($P < 0.002$). On the fascial surfaces, there did not appear to be any relationship between the baseline level of hypoxia and the magnitude of reduction in HP (Fig. 5).

On the tumor surfaces, individual experiments showed both increases and decreases in HP after treatment with sugar and oxygen (Fig. 5). For mannitol, the HP remained virtually unchanged; the median difference between baseline and during oxygen breathing was an increase of 0.8%, which was not significant ($P = 1.00$). For glucose, the results were similar. The HP was reduced by 10%, but this difference was not significant ($P = 0.44$). When the results of the

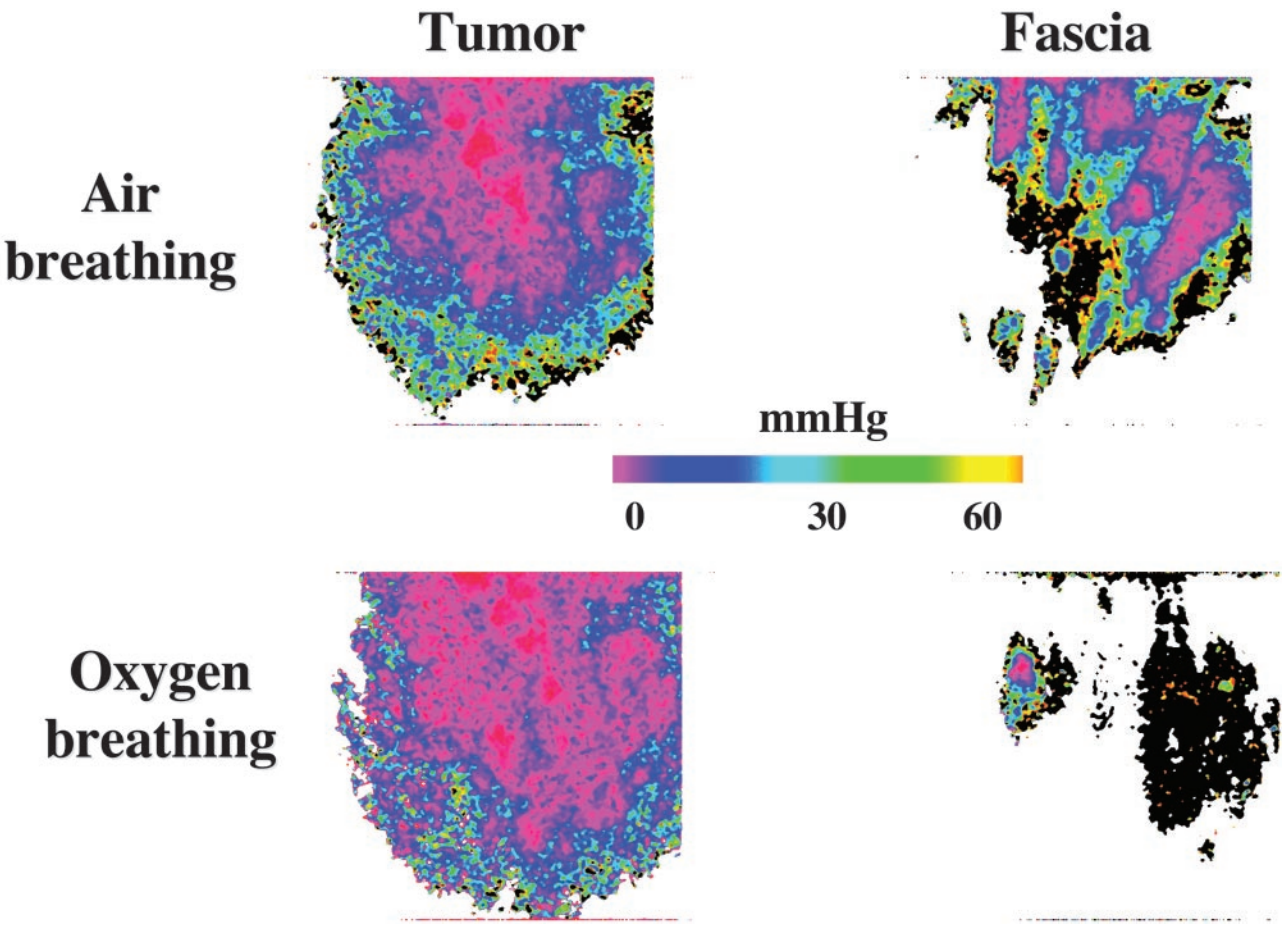

Fig. 3. Phosphorescence lifetime images from one experiment, before and 30 min after mannitol, during O_2 breathing. The HP decreases on the fascial surface after manipulation, whereas the tumor surface becomes slightly more hypoxic. The *color bar* in the center of the figure indicates color range *versus* pO_2.

two sugars were combined, the HP decreased by a median of 4.2%, which was also not significant ($P = 0.54$).

DISCUSSION

There have been numerous attempts to improve oxygenation of tumors, using a variety of methods in both preclinical models and in clinical trials. Many of these prior studies have been reviewed comprehensively (17, 18). Although some of the methods have shown success, systematic and serial evaluation of such manipulations in models in which the underlying physiology is well defined, quantitatively on a microregional level has yet to be performed. For example, Fenton *et al.* (19, 20) have studied the effects of methods to alter tumor oxygenation in physiologically defined tumor models using cyrospectrophotometry combined with hypoxia marker drugs and perfusion marker dyes. These studies have been informative, but serial measurements have not been possible, which eliminates the ability to assess individual differences in tumor response to manipulation. Additionally, no clinical study has yet overwhelmingly shown the value of improving oxygenation as a means to improve tumor response or local control after radiation or chemotherapy, although oxygen is well known to be a powerful modifier of both. Well-defined tumor physiological models may lead to better methods for manipulation because multiple parameters can be measured, thereby increasing the likelihood that an explanation for failure/or success can be identified.

This is the first study that has serially examined the effects of manipulation of oxygenation in a model where regional characteristics of oxygen delivery and metabolism are well defined. This model has the advantage of allowing comparison of the responses to manipulation of two regions that differ greatly with respect to features of tumor physiology that are important for oxygen transport. These two regions have some similarities to regions that would be found in larger three-dimensional tumors. There are clear differences in vascular density, proximity to feeding arterioles, vascular oxygenation, and dominance of aerobic *versus* anaerobic metabolism.

In prior studies with this model, we found that the arteriolar supply to these tumors emerges from the underlying fascia (21) and the vascular density on the fascial surface is significantly higher than on the tumor surface (6). The magnetic resonance angiography results in this study independently validate this difference in vessel density. We have previously shown that the fascial arterioles vasoconstrict in response to hemoglobin scavengers (22) and hypercarbic gases such as carbogen (16). They do not react to O_2 breathing, which is why we chose O_2 breathing for these studies (16). They also vasoconstrict in response to NO scavengers (22) but do not dilate in response to NO donors (23). The differences in supply lead to higher vascular oxygenation on the fascial *versus* the tumor surfaces under baseline conditions (4, 5, 21).

Table 1 *Comparison of fascial versus tumor surfaces at baseline*[a]

Surface	*n*	Maximum	Median	Minimum	25th percentile	75th percentile
Fascia	17	59.3	6.0	0.1	1.2	14.3
Tumor	17	82.3	27.9	0.4	9.0	54.4

[a] The difference between fascial and tumor surfaces was significant ($P = 0.0002$).

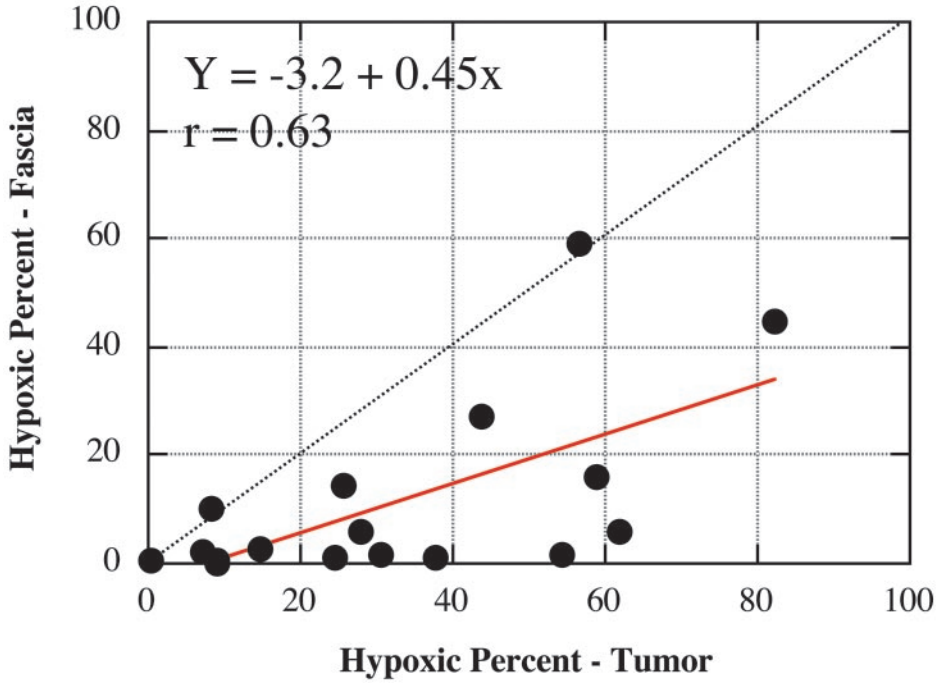

Fig. 4. Comparison of pretreatment HP for tumor *versus* fascial surfaces. There was a significant relationship between the two parameters, indicating that more poorly oxygenated tumors showed evidence for more hypoxia on both tissue surfaces. The linear regression fit to the data are shown ($P = 0.0067$). For most tumors, the HP on the tumor surface is higher than on the fascial surface, *Dashed line* = line of identity.

Blood flow in vessels on the tumor surface varies temporally, and this variation affects vascular and tissue pO_2 (24). Temporal variation in flow has been observed on the fascial surface as well (M. W. Dewhirst, unpublished data).

In this article, the HP on tumor surfaces averaged 20% higher than on fascial surfaces, which is virtually identical to our previous results for this tumor model in independent studies with PLI (4). More recently, we found gradients of glucose and lactate that mirror the gradient in oxygenation (6). Specifically, the tumor surface has relatively high concentrations of lactate and low concentrations of glucose, relative to the fascial surface. This is consistent with a transition from aerobic to anaerobic metabolism.

The purpose of this study was to compare the effects of oxygen transport manipulation protocols (mannitol + O_2 *versus* glucose + O_2) on HP of the fascial and tumor surfaces. This study was stimulated by an earlier report showing significant improvements in pO_2 of this tumor line when grown in the flank using the combination of hyperglycemia with oxygen breathing (7). The combination of glucose and oxygen breathing was shown to be better than either manipulation alone at increasing tumor pO_2. However, when baseline pO_2 was near 0, there was little effect of O_2 breathing with or without hyperglycemia. This led us to speculate that very hypoxic tumor regions may be refractory to oxygen manipulation.

We hypothesized that tumor surfaces of the skin-fold window chamber might represent regions that are refractory to oxygen manipulation. The results are consistent with our prior studies with microelectrode measurements in flank tumors (7). In the flank tumor study, we observed both increases and decreases in pO_2 after manipulation in regions with low baseline pO_2 (7). The net effect was very little change in overall pO_2 when the baseline was low. We observed the same phenomenon here for the tumor surface.

The results of this work support the hypothesis that the tumor surface is refractory to improving pO_2 by this method. We found that the HP tended to show random fluctuation on the tumor surface after manipulation (Fig. 5), which may have been because of fluctuations in vascular perfusion and/or red cell flux, as we have demonstrated previously for this tumor model (24). In comparison, there were few instances of increased HP after manipulation on the fascial surface of the tumor window, which started out with a relatively low HP, on average. However, there was considerable overlap in baseline HP between the tumor and fascial surfaces when comparing across the population of tumors (Fig. 5). We interpret this to mean that hypoxic regions of tumor with adequate vascular supply or those near arteriolar sources are more easily reoxygenated by manipulation of oxygen transport. Furthermore, we know that flow fluctuations occur in such regions, just as they do on the tumor surface, yet these fluctuations must have been relatively unimportant in influencing oxygen transport when animals were breathing oxygen.

There are several potential mechanisms for the resistance of the tumor surface to reoxygenation. First, it is possible that glucose did

Table 2 *Comparison of hypoxic percentiles before and after manipulation for each sugar alone and for combined data*

	Mannitol				Glucose				Combined			
	Fascia		Tumor		Fascia		Tumor		Fascia		Tumor	
Hypoxic %	*n*	Median (IQR)	*n*	Median (IQR)	*n*	Median (IQR)	*n*	Median (IQR)	*n*	Median (IQR)	*n*	Median (IQR)
Baseline (air)	7	6.1 (0.4:14.8)	7	14.6 (8.9:27.9)	6	4.0 (1.7:44.9)	6	55.6 (37.8:62.1)	13	6.0 (1.7:14.3)	13	27.9 (9.0:54.4)
After sugar	NA	NA	6[b]	21.5 (17.1:29.0)	NA	NA	5*	50.5 (41.7:58.5)	NA	NA	11*	36.1 (18.8:50.5)
During O_2	7	0.4 (0.1:2.3)	7	16 (13.7:31.2)	6	1.1 (0.1:1.8)	6	42.7 (29.6:56.6)	13	0.5 (0.1:1.8)	13	29.6 (14.5:35.5)

[a] IQR, interquartile range (25^{th} percentile: 75^{th} percentile); NA, not applicable.

[b] Two experiments were missing data points after sugar alone because of technical problems during the experiment. Measurements were available, however, during O_2 breathing of the same experiments, which commenced after the sugar infusion was completed. Measurements of the fascial surface were not made during glucose infusion so that the tumor surface could be continuously monitored without moving the animal. Statistical comparisons are in Table 3.

Table 3 *Statistical comparisons of hypoxic fraction within tumor surface over time or between tumor surfaces after treatment*[a]

Manipulation (*n*)	Posttreatment Tumor *versus* Fascia[b]		Fascia		Tumor	
			Post *versus* baseline		Post *versus* baseline	
	Avg. difference in hypoxic % (tumor-fascia)	*P*	Avg. difference in hypoxic % (postbaseline)	*P*	Avg. difference in hypoxic % (postbaseline)	*P*
Mannitol (6)	ND[c]	ND	ND	ND	2	0.56
Mannitol + O_2 (7)	−18	0.02	−6	0.03	1	1.00
Glucose* (5)	ND	ND	ND	ND	−6	0.44
Glucose + O_2 (6)	−33	0.03	−13	0.06	−10	0.44
Combined sugars[d] (11)	ND	ND	ND	ND	−2	0.97
Combined Sugars + O_2 (13)	−25	0.0002	−9	0.002	−4	0.54

[a] *P* was based on the signed rank test.
[b] Pre Tumor *versus* Fascia comparison of hypoxic fraction was done using all the data from all the groups: the average difference in hypoxic % (Tumor-Fascia) = −21 and $P = 0.0002$ ($n = 17$, including the glucose only group).
[c] ND = Study not done.
[d] Data from four mice of glucose only group were not included.

not reach the oxygen consuming regions of this tumor model in high enough concentrations to reduce oxygen consumption via the Crabtree effect. Mathematical models based on prior experimental data with this model suggest that a 30% reduction in oxygen consumption rate would be sufficient to eliminate hypoxia (10, 11). Prior *in vitro* studies with this tumor line show that 5 mM tissue glucose reduces O_2 consumption by 50%, thus being sufficient to improve tumor oxygenation (7). However, in *in vivo* studies, hyperglycemia alone induced only mild improvements in pO_2, whereas the combination of hyperglycemia with O_2 breathing yielded supra-additive effects. It is possible under this circumstance that hyperglycemia achieved a heterogeneous and suboptimal Crabtree effect; thus, the combination with oxygen breathing was sufficient overall to efficiently reduce hypoxia in most of the tumor tissue. Tissue and interstitial fluid glucose concentrations in this model average 3.5 mM (6) and 0.15 mM (25) under baseline conditions, respectively. Is it not known whether levels >5 mM are reached within these tumors upon induction of hyperglycemia at the dose of glucose used. Experiments are currently underway to address this issue. In any case, it is likely that the degree of improvement in glucose concentrations will be heterogeneous because glucose concentrations at baseline are heterogeneous (6).

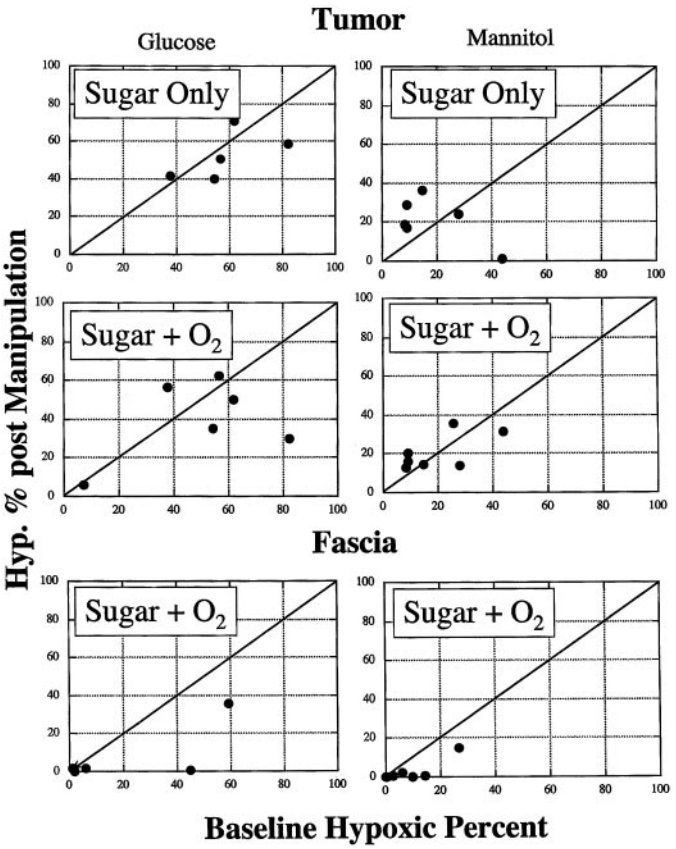

Fig. 5. Comparison of HP posttreatment *versus* pretreatment for tumor and fascial surfaces. Results from individual experiments are shown. ● = sugar + O_2 breathing, ○ = sugar alone. *Lines* = line of identity. For the tumor surfaces, the data after manipulation are scattered on both sides of the identity line, indicating no predictable effect of manipulation on pO_2. On the fascial surface, the data clearly show that HP is reduced after manipulation.

Mannitol and glucose pretreatment before oxygen breathing had similar effects on fascial surface pO_2 during oxygen breathing, and mannitol is an unmetabolizable sugar. This would suggest that the Crabtree effect was not efficiently induced. Otherwise, the pO_2 of animals treated with glucose should have increased more than with mannitol. Additional studies in this laboratory are investigating factors that control glucose transport and metabolism in this tumor to test whether they could contribute to inefficiencies in inducing the Crabtree effect. This tumor line is sensitive to the Crabtree effect *in vitro* under normoxic conditions at pH 7.3, but chronically acidified tumor cells may not be as sensitive, thereby making the tumor less sensitive to the Crabtree effect (26).

An alternative explanation for the similarities in effect between glucose and mannitol might be related to effects on blood volume because both sugars could cause hyperosmolarity. This explanation is unlikely, however, for two reasons. First, in prior studies, we demonstrated that the effect of glucose in improving tumor oxygenation occurs within 1–2 min after infusion of the sugar, but it lasts far beyond the period of hyperglycemia (blood glucose drops to baseline ~30 min after completion of the infusion, but the improvement in tumor pO_2 lasts out to 60 min after glucose infusion; Ref. 7). Second, we did not find any effect of hyperglycemia on hematocrit (data not shown); if hyperosmolarity occurred, hemodilution could be a measurable result. Third, there was no measurable effect of hyperglycemia at the dose used in this study on blood pressure or tumor perfusion (7). When a 4-fold higher dose of glucose was used (4 g/kg instead of 1 g/kg used in this work), tumor blood flow was significantly reduced in this same tumor model (7). This latter effect was likely attributable to rheological changes because glucose has been shown to increase red cell rigidity (27). Thus, any rheological effect of hyperglycemia would increase blood viscosity, thereby leading to a reduction in tumor perfusion and pO_2. The reduction in pH that accompanies hyperglycemia would contribute additionally to increases in red cell rigidity (28). It is unlikely that these effects are created by any systemic effect of the anesthesia used. We have shown previously that the method of anesthesia used in this article yields average blood pressures and blood gas values that are in the normal range for awake animals (21).

It is important to consider what options might be available to additionally improve the oxygenation of refractory regions such as the tumor surface. One option would be to consider additional pharmacological approaches to additionally reduce oxygen consumption. Drugs such as meta-iodo-benzylguanidine, the inhibitor of site I of oxidative phosphorylation, have this potential (29). Recently, it has been shown that the combination of meta-iodo-benzylguanidine and hyperglycemia was very efficient in reducing hypoxia in human melanoma xenografts (30). Another approach that has shown promise recently is to use agents that right-shift the hemoglobin saturation curve in combination with hyperoxic gas breathing (31, 32).

Consideration of other pathophysiological features of oxygen transport on the tumor surface suggests an additional option that is worth reconsidering, namely, manipulation of red cell rigidity. We have previously shown that vascular pO_2 on the tumor surface averages 2-fold lower (12 mm Hg on average; Ref. 5) than on the fascial surface (30 mm Hg, on average; Ref. 21) and that a significant fraction of vessels on the tumor surface have active flow but are functionally hypoxic (*i.e.,* all oxygen has been delivered before the red cells reach vessels near the tumor surface; Ref. 5). Furthermore, at least 10% of the vessels on this surface are devoid of red cells despite having active plasma flow (33). Conditions simulating the intravascular hypoxia in this tumor lead to slight crenation of red cells, thereby increasing red cell suspension viscosity and a tendency toward rouleau formation (28). The increase in viscosity augments flow resistance, thereby reducing flow velocity and perfusion. It is highly likely that the increase in viscosity also promotes uneven distribution of red cells at vessel bifurcation points, leading to a propensity for plasma channels. In prior studies, it has been demonstrated that calcium channel blockers can reverse the rheological effects of hypoxia and improve perfusion and oxygenation of the tumor surface (34). Other studies with similar drugs showed improvements in radiation response of murine tumor lines (35, 36). Despite early success with this class of drugs in preclinical models, this approach was never tested clinically. Use of calcium channel blockers, in combination with manipulation of oxygenation, would attack two fundamental limitations of oxygen delivery based on independent, defined pathophysiological features of tumor microcirculation.

Because the window chamber tumor model represents an unusual vascular arrangement, it is important to consider whether regions refractory to oxygenation can be seen in larger three-dimensional tumors. Several sets of data suggest that this is the case. Hunjan *et al.* (37) used ^{19}F nuclear magnetic resonance spectroscopy of hexafluorobenzene injected into Dunning prostate tumors transplanted into rats. When they examined the pO_2 of central tumor regions, they found relatively little effect of hyperoxic gas breathing on pO_2, whereas peripheral tumor regions were easily manipulated to higher pO_2 values. One could imagine that the central portions of these tumors were furthest removed from the arteriolar source, but careful validation would be needed to verify that. Similarly, Krishna *et al.* (38) used Overhauser-enhanced magnetic resonance imaging of an oxygen-sensitive spin trap to assess changes in tumor pO_2 after hyperoxic gas breathing. They also found regions of transplanted tumors that were refractory to manipulation by carbogen breathing. In this case, the regions were not always in the center of tumors.

Examination of data from published human studies show trends similar to that described herein for these murine models. For example, Falk *et al.* (39) examined pO_2 distributions, using Eppendorf PO2 histography, in 17 patients with head and neck cancer before and during carbogen breathing. Although they observed significant improvements in median pO_2, they were much less successful in eliminating the HP (defined in this study as proportion of measurements < 2.5 mm Hg). Four tumors showed no improvement in pO_2 upon carbogen breathing, and in the 11 patients in whom the median pO_2 was successfully improved, the HP was only eliminated in 3. Similar results in human patients have been reported by Guichard *et al.* (40), Laurence *et al.* (41), and Martin *et al.* (42).

Griffiths *et al.* (43) used gradient-recalled echo magnetic resonance imaging to assess changes in perfusion/hemoglobin saturation in 31 human primary or metastatic tumors after the switch from air to carbogen breathing. Eleven tumors (35%) failed to show improvement in signal intensity, indicating probable lack of improvement in perfusion and/or pO_2. The magnitude of the effect was variable in the remaining patients. Some caution needs to be exercised in interpretation of these data because the signal change that is monitored is sensitive to both perfusion and changes in hemoglobin oxygen saturation. Recent studies by our group have also shown the signal to be sensitive to changes in microvessel red cell hematocrit, which can be altered by vasoactive gases such as carbogen (16, 44).

The radiobiological significance of tumor regions that are refractory to reoxygenation by manipulation is not known. It is possible that such regions are necrotic, although this is clearly not the case for the skin-fold window chamber model of the tumor used in this study. The tumor surface of this model contains histologically viable tumor cells admixed with regions of squamous metaplasia (6).

In summary, the results of this study confirm the hypothesis that tumor regions that have low vascular pO_2 and high levels of anaerobic metabolism are refractory to manipulation of oxygenation by breathing oxygen with or without glucose. The well-defined characteristics of this tumor model make it ideally suited for examining different strategies for improving oxygenation of such refractory regions. Examples of such strategies have been proposed for future investigation.

ACKNOWLEDGEMENTS

We thank the Duke In Vivo Microscopy Center (P4105959) in obtaining the magnetic resonance angiography data depicted in this study. We also thank Isabel Cardenas Navia for her assistance in the preparation of this article.

REFERENCES

1. Thomlinson, R., and Gray, L. The histological structure of some human lung cancers and the possible implications for radiotherapy. Br. J. Cancer, *9:* 539–549, 1955.
2. Dewhirst, M. W. Concepts of oxygen transport at the microcirculatory level. Semin. Radiat. Oncol., *8:* 143–150, 1998.
3. Helmlinger, G., Yuan, F., Dellian, M., and Jain, R. Interstitial pH and pO_2 gradients in solid tumors *in vivo*: high resolution measurements reveal a lack of correlation. Nat. Med., *3:* 177–182, 1997.
4. Dewhirst, M. W., Ong, E. T., Braun, R. D., Smith, B., Klitzman, B., Evans, S. M., and Wilson, D. Quantification of longitudinal tissue pO_2 gradients in window chamber tumours: impact on tumour hypoxia. Br. J. Cancer, *79:* 1717–1722, 1999.
5. Dewhirst, M. W., Ong, E. T., Klitzman, B., Secomb, T. W., Vinuya, R. Z., Dodge, R., Brizel, D., and Gross, J. F. Perivascular oxygen tensions in a transplantable mammary tumor growing in a dorsal flap window chamber. Radiat. Res., *130:* 171–182, 1992.
6. Walenta, S., Snyder, S., Haroon, Z. A., Braun, R. D., Amin, K., Brizel, D., Mueller-Klieser, W., Chance, B., and Dewhirst, M. W. Tissue gradients of energy metabolites mirror oxygen tension gradients in a rat mammary carcinoma model. Int. J. Radiat. Oncol. Biol. Phys., *51:* 840–848, 2001.
7. Snyder, S. A., Lanzen, J. L., Braun, R. D., Rosner, G., Secomb, T. W., Biaglow, J., Brizel, D. M., and Dewhirst, M. W. Simultaneous administration of glucose and hyperoxic gas achieves greater improvement in tumor oxygenation than hyperoxic gas alone. Int. J. Radiat. Oncol. Biol. Phys., *51:* 494–506, 2001.
8. Crabtree, H. LXI. Observations on the carbohydrate metabolism of tumours. Biochem. J., *23:* 536–545, 1929.
9. Wojtcak, L. The Crabtree effect: a new look at the old problem. Acta Biochemica Polonica, *42:* 361–368, 1996.
10. Secomb, T. W., Hsu, R., Ong, E. T., Gross, J. F., and Dewhirst, M. W. Analysis of the effects of oxygen supply and demand on hypoxic fraction in tumors. Acta Oncol., *34:* 313–316, 1995.
11. Secomb, T. W., Hsu, R., Braun, R. D., Ross, J. R., Gross, J. F., and Dewhirst, M. W. Theoretical simulation of oxygen transport to tumors by three-dimensional networks of microvessels. Adv. Exp. Med. Biol., *454:* 629–634, 1998.
12. Papenfuss, D., Gross, J., Intaglietta, M., and Treese, F. A transparent access chamber for the rat dorsal skin fold. Microvasc. Res., *18:* 311–318, 1979.
13. Wilson, D., and Cerniglia, G. Oxygenation of tumors as evaluated by phosphorescence imaging. Adv. Exp. Med. Biol., *345:* 539–547, 1994.

14. Wilson, D. F., Evans, S. M., Jenkins, W. T., Vinogradov, S. A., Ong, E., and Dewhirst, M. W. Oxygen distributions within R3230Ac tumors growing in dorsal flap window chambers in rats. Adv. Exp. Med. Biol., *454:* 603–609, 1998.
15. Vinogradov, S., Lo, L., Jenkins, W., Evans, S., Koch, C., and Wilson, D. Non-invasive imaging of the distribution of oxygen in tissue *in vivo* using near infra-red phosphors. Biophys. J., *70:* 1609–1617, 1996.
16. Dunn, T. J., Braun, R. D., Rhemus, W. E., Rosner, G. L., Secomb, T. W., Tozer, G. M., Chaplin, D. J., and Dewhirst, M. W. The effects of hyperoxic and hypercarbic gases on tumour blood flow. Br. J. Cancer, *80:* 117–126, 1999.
17. Vaupel, P., Kelleher, D. K., and Thews, O. Modulation of tumor oxygenation. Int. J. Radiat. Oncol. Biol. Phys., *42:* 843–848, 1998.
18. Overgaard, J., and Horsman, M. Modification of hypoxia-induced radioresistance in tumors by use of oxygen and sensitizers. Semin. Radiat. Oncol., *6:* 10–21, 1996.
19. Fenton, B. M. Influence of hydralazine administration on oxygenation in spontaneous and transplanted tumor models. Int. J. Radiat. Oncol. Biol. Phys., *49:* 799–808, 2001.
20. Fenton, B. M., Lord, E. M., and Paoni, S. F. Enhancement of tumor perfusion and oxygenation by carbogen and nicotinamide during single- and multifraction irradiation. Radiat. Res., *153:* 75–83, 2000.
21. Dewhirst, M., Ong, E., Rosner, G., Rehmus, S., Shan, S., Braun, R., Brizel, D., and Secomb, T. Arteriolar oxygenation in tumor and subcutaneous arterioles: effects of inspired air oxygen content. Br. J. Cancer, *74:* S241–S246, 1996.
22. Hahn, J. S., Braun, R. D., Dewhirst, M. W., Shan, S., Snyder, S. A., Taube, J. M., Ong, E. T., Rosner, G. L., Dodge, R. K., Bonaventura, J., Bonaventura, C., DeAngelo, J., and Meyer, R. E. Stroma-free human hemoglobin A decreases R3230Ac rat mammary adenocarcinoma blood flow and oxygen partial pressure. Radiat. Res., *147:* 185–194, 1997.
23. Shan, S. Q., Rosner, G. L., Braun, R. D., Hahn, J., Pearce, C., and Dewhirst, M. W. Effects of diethylamine/nitric oxide on blood perfusion and oxygenation in the R3230Ac mammary carcinoma. Br. J. Cancer, *76:* 429–437, 1997.
24. Kimura, H., Braun, R. D., Ong, E. T., Hsu, R., Secomb, T. W., Papahadjopoulos, D., Hong, K., and Dewhirst, M. W. Fluctuations in red cell flux in tumor microvessels can lead to transient hypoxia and reoxygenation in tumor parenchyma. Cancer Res., *56:* 5522–5528, 1996.
25. Ettinger, S. N., Poellmann, C. C., Wisniewski, N. A., Gaskin, A. A., Shoemaker, J. S., Poulson, J. M., Dewhirst, M. W., and Klitzman, B. Urea as a recovery marker for quantitative assessment of tumor interstitial solutes with microdialysis. Cancer Res., *61:* 7964–7970, 2001.
26. Burd, R., Wachsberger, P. R., Biaglow, J. E., Wahl, M. L., Lee, I., and Leeper, D. B. Absence of Crabtree effect in human melanoma cells adapted to growth at low pH: reversal by respiratory inhibitors. Cancer Res., *61:* 5630–5635, 2001.
27. Traykov, T. T., and Jain, R. K. Effect of glucose and galactose on red blood cell membrane deformability. Int. J. Microcirc. Clin. Exp., *6:* 35–44, 1987.
28. Kavanagh, B., Coffey, B., Needham, D., Hochmuth, R., and Dewhirst, M. The effect of flunarizine on erythrocyte suspension viscosity under conditions of extreme hypoxia, low pH and lactate treatment. Br. J. Cancer, *67:* 734–741, 1993.
29. Biaglow, J. E., Manevich, Y., Leeper, D., Chance, B., Dewhirst, M. W., Jenkins, W. T., Tuttle, S. W., Wroblewski, K., Glickson, J. D., Stevens, C., and Evans, S. M. MIBG inhibits respiration: potential for radio- and hyperthermic sensitization. Int. J. Radiat. Oncol. Biol. Phys., *42:* 871–876, 1998.
30. Burd, R., Lavorgna, S. N., Daskalakis, C., Wachsberger, P. R., Wahl, M. L., Biaglow, J. E., Stevens, C. W., and Leeper, D. B. Tumor oxygenation and acidification are increased in melanoma xenografts after exposure to hyperglycemia and meta-iodobenzylguanidine. Radiat. Res., *159:* 328–335, 2003.
31. Kavanagh, B. D., Khandelwal, S. R., Schmidt-Ullrich, R. K., Roberts, J. D., Shaw, E. G., Pearlman, A. D., Venitz, J., Dusenbery, K. E., Abraham, D. J., and Gerber, M. J. A Phase I study of RSR13, a radiation-enhancing hemoglobin modifier: tolerance of repeated intravenous doses and correlation of pharmacokinetics with pharmacodynamics. Int. J. Radiat. Oncol. Biol. Phys., *49:* 1133–1139, 2001.
32. Kavanagh, B. D., Secomb, T. W., Hsu, R., Lin, P. S., Venitz, J., and Dewhirst, M. W. A theoretical model for the effects of reduced hemoglobin-oxygen affinity on tumor oxygenation. Int. J. Radiat. Oncol. Biol. Phys., *53:* 172–179, 2002.
33. Dewhirst, M., Kimura, H., Rehmus, S., Braun, R., Papahadjopoulos, D., Hong, K., and Secomb, T. Microvascular studies on the origins of perfusion-limited hypoxia. Br. J. Cancer, *74:* S247–S251, 1996.
34. Dewhirst, M. W., Ong, E. T., Madwed, D., Klitzman, B., Secomb, T., Brizel, D., Bonaventura, J., Rosner, G., Kavanagh, B., Edwards, J., *et al*. Effects of the calcium channel blocker flunarizine on the hemodynamics and oxygenation of tumor microvasculature. Radiat Res, *132:* 61–68, 1992.
35. Wood, P. J., and Hirst, D. G. Cinnarizine and flunarizine improve the tumour radiosensitisation induced by erythrocyte transfusion in anaemic mice. Br. J. Cancer, *60:* 36–40, 1989.
36. Wood, P. J., and Hirst, D. G. Cinnarizine and flunarizine as radiation sensitisers in two murine tumours. Br. J. Cancer, *58:* 742–745, 1988.
37. Hunjan, S., Mason, R. P., Constantinescu, A., Peschke, P., Hahn, E. W., and Antich, P. P. Regional tumor oximetry: 19F NMR spectroscopy of hexafluorobenzene. Int. J. Radiat. Oncol. Biol. Phys., *41:* 161–171, 1998.
38. Krishna, M. C., English, S., Yamada, K., Yoo, J., Murugesan, R., Devasahayam, N., Cook, J. A., Golman, K., Ardenkjaer-Larsen, J. H., Subramanian, S., and Mitchell, J. B. Overhauser enhanced magnetic resonance imaging for tumor oximetry: coregistration of tumor anatomy and tissue oxygen concentration. Proc. Natl. Acad. Sci. USA, *99:* 2216–2221, 2002.
39. Falk, S. J., Ward, R., and Bleehen, N. M. The influence of carbogen breathing on tumour tissue oxygenation in man evaluated by computerised pO_2 histography. Br. J. Cancer, *66:* 919–924, 1992.
40. Guichard, M., Lartigau, E., Martin, L., Thomas, C., Weeger, P., Lambin, P., Le Ridant, A. M., Lusinchi, A., Wibault, P., Luboinski, B., *et al*. Tumor oxygenation after 1) carbogen and/or perflubron emulsion administration in tumor xenografts 2) carbogen administration in patients. Artif. Cells Blood Substit. Immobil. Biotechnol., *22:* 1355–1360, 1994.
41. Laurence, V. M., Ward, R., Dennis, I. F., and Bleehen, N. M. Carbogen breathing with nicotinamide improves the oxygen status of tumours in patients. Br. J. Cancer, *72:* 198–205, 1995.
42. Martin, L., Lartigau, E., Weeger, P., Lambin, P., Le Ridant, A. M., Lusinchi, A., Wibault, P., Eschwege, F., Luboinski, B., and Guichard, M. Changes in the oxygenation of head and neck tumors during carbogen breathing. Radiother. Oncol., *27:* 123–130, 1993.
43. Griffiths, J. R., Taylor, N. J., Howe, F. A., Saunders, M. I., Robinson, S. P., Hoskin, P. J., Powell, M. E., Thoumine, M., Caine, L. A., and Baddeley, H. The response of human tumors to carbogen breathing, monitored by Gradient-Recalled Echo Magnetic Resonance Imaging. Int. J. Radiat. Oncol. Biol. Phys., *39:* 697–701, 1997.
44. Neeman, M., Dafni, H., Bukhari, O., Braun, R. D., and Dewhirst, M. W. *In vivo* BOLD contrast MRI mapping of subcutaneous vascular function and maturation: validation by intravital microscopy. Magn. Reson. Med., *45:* 887–898, 2001.